RELATION BETWEEN STRUCTURAL DISORDER AND OTHER CHARACTERISTICS OF KAOLINITES AND DICKITES

G. W. Brindley,[†] Chih-Chun Kao[1]

Mineral Sciences Building, The Pennsylvania State University
University Park, Pennsylvania 16802

J. L. Harrison
Georgia Kaolin Research, Springfield, New Jersey 07081

M. Lipsicas[2] and R. Raythatha
Schlumberger-Doll Research, Ridgefield, Connecticut 06877

Abstract—A suite of Georgia kaolinites, ranging from well-ordered to very poorly ordered samples, were studied to explore correlations between degree of structural disorder, geological environment, Fe^{3+} content, Fe^{3+} electron paramagnetic resonance (EPR) spectrum, and infrared (IR) hydroxyl-stretching band frequencies and bandwidths. Samples from different localities showed a wide range of disorder which appears to be related to differences in their geological environments. High iron content correlated strongly with low degree of order. The areas of both the I and E components of the EPR spectrum and the fractional I area correlated inversely with degree of order. Fourier-transform IR studies of kaolinites and dickites showed that (1) interlayer hydrogen bonding is weaker in dickite than in kaolinite; (2) frequency of the ν_1 stretching band of the inner-surface hydroxyls increases sequentially from well-ordered kaolinite through the disordered structures to well-ordered dickite, which is consistent with a model for disorder based on vacancy displacement; and (3) the character and temperature dependence of the inner hydroxyl-stretching band is not compatible with the crystal structures of kaolinite and dickite as refined by Suitch and Young.

Key Words—Crystallinity, Dickite, Disorder, Electron paramagnetic resonance, Fourier-transform infrared spectroscopy, Kaolinite.

INTRODUCTION

Kaolinite and dickite are dioctahedral 1:1 layer silicates. The structure of kaolinite has been studied by Brindley and Robinson (1946), Brindley and Nakahira (1958), Zvyagin (1960), Giese (1982), Adams (1983), and Suitch and Young (1983). The structure of dickite has been examined by Newnham and Brindley (1956, 1957), Newnham (1961), Giese and Datta (1973), and Adams and Hewat (1981). Bailey (1963) demonstrated that both kaolinite and dickite are based on a $1M$ stacking sequence of layers, and that the minerals would be identical if they were trioctahedral. The two structures differ mainly in the distribution of the vacant octahedral sites which, in the notation of Bailey, are wholly B or wholly C in every layer in kaolinite and alternately B and C in successive layers in dickite.

The two minerals have various degrees of structural disorder or "crystallinity" produced either by geological conditions of formation, transport, or deposition,

or by mechanical treatment such as grinding. In this report, the term "degree of disorder" is used rather than "crystallinity." "Crystallinity" has generally been used in the past to refer either to the fraction of crystalline material in a mixture of crystalline and noncrystalline materials or crystallite size. In the present study, dioctahedral 1:1 phases containing various amounts of material having kaolinite and dickite characteristics, both of which are wholly crystalline, have been examined. Therefore, degree of disorder is a more appropriate term than crystallinity.

Plançon and Tchoubar (1977a, 1977b), and Tchoubar *et al.* (1982) made detailed calculations in which models of structural disorder were correlated with X-ray powder diffraction line profiles. They established that the principal type of disorder in natural kaolinites is the displacement from one layer to another of the vacant octahedral sites. Stacking faults by translation of $\pm b/3$ appeared to play a minor role. Rotation of layers was rejected as a significant kind of disorder in kaolinite. Brindley and Porter (1978) observed that a "mistake" in the dickite sequence of vacant sites introduces a kaolinite component and that a "mistake" in the kaolinite sequence introduces a dickite component. They described variously disordered dickites which in the most disordered forms were almost in-

---

† Deceased October 23, 1983.
[1] Present address: Department of Materials Engineering, Tatung Institute of Technology, Taipei, Taiwan, Republic of China.
[2] To whom all correspondence should be addressed.

239

distinguishable from disordered kaolinites insofar as their X-ray powder diffractograms were concerned.

The correlation between the degree of disorder in kaolinites and iron content is well known. Furthermore, Angel *et al.* (1974), Jones *et al.* (1974), Meads and Malden (1975), and Mestdagh *et al.* (1980) studied the relationship in kaolinite between structural iron content and degree of disorder using electron paramagnetic resonance spectroscopy (EPR). The EPR signal of kaolinite in the range g = 3–5 has been shown (Angel *et al.*, 1974; Jones *et al.*, 1974) to be due to Fe^{3+} ions in the high spin state (S = 5/2). It consists of four lines, an approximately isotropic line I at $g_I \approx 4.2$ and triplet E with components at $g_z \approx 4.7$, $g_x \approx 3.8$, and $g_y \approx 3.4$ (Hall, 1973). Components g_x and g_y were only resolved at temperatures below about 120 K. The I line is due to Fe^{3+} ions at a site having orthorhombic symmetry, and the E lines to Fe^{3+} ions at a site of higher symmetry (Hall, 1973; Jones *et al.*, 1974; Meads and Malden, 1975). Both sites are presumably in the octahedral sheet, where Fe^{3+} replaces Al^{3+}.

Mestdagh *et al.* (1982) postulated an interdependence between the proportion of defects due to an octahedral vacancy displacement, the concentration of Fe^{3+} in the I site, and the ratio of intensities of two of the hydroxyl-stretching bands of the IR spectrum. Cruz-Cumplido *et al.* (1982) claimed that the IR spectral characteristics and the cohesion energy in kaolinites are intimately related to the orientation of the hydroxyls, which they believed was controlled by the distribution of the Al vacancies in successive layers. An inverse relation between the degree of order and the interlamellar cohesion energy was indicated on the basis of hydrazine intercalation experiments.

The objective of the present study was to determine whether the degree of disorder of a 1:1 clay was related to its geological environment, the amount of structural Fe^{3+} present, the details of the Fe^{3+} EPR spectrum, or the details of hydroxyl-stretching bands in its IR spectrum. This study differed from previous studies in that it: (1) examined a wide range of kaolinites and dickites with varying degrees of disorder (most of the kaolinites studied were a suite of Georgia kaolinites); (2) used a Fourier-transform IR spectrometer which yielded a considerably greater signal to noise ratio than could be obtained with an ordinary prism or grating IR spectrometer; and (3) employed deconvolution programs for IR and EPR data reduction. By these means, the individual IR frequencies in the range of interest were obtained directly along with their integrated absorbances (i.e., peak areas) and the half-widths of the peaks. The resulting data permitted a more detailed discussion of bandwidths and frequencies of the different hydroxyl-stretching bands than was possible in previous studies. The deconvolution program provided a detailed analysis of the Fe^{3+} spectra due to structural iron in the Georgia kaolinite samples.

EXPERIMENTAL

Materials

Table 1 lists the source, total Fe_2O_3 content, particle size index, and Hinckley index of the sample studied. The sample abbreviations listed in this table are used throughout the paper.

Six kaolinites were obtained from the Georgia Kaolin Company, each of which consisted of 2–4 samples of different particle size distribution. The Georgia specimens were from five different localities, as indicated in Table 1. These samples were ideal for an IR study of the degree of disorder because (1) they required little or no mechanical treatment and hence grinding effects could be minimized, and (2) the particle size effect could be minimized by studying samples having similar particle size distributions.

Kaolinites from Keokuk, Iowa, and Shelbina, Missouri, were provided by Dr. W. D. Keller. The Keokuk sample is an exceptionally well-ordered geode kaolinite and has been discussed by Keller *et al.* (1966), Brindley and Porter (1978), and Suitch and Young (1983). The Shelbina sample, another exceptionally well-ordered kaolinite, occurs in small vugs in the Mississippian-age Chouteau limestone near Shelbina, Shelby County, northeast Missouri (W. D. Keller, University of Missouri, 305 Geology Building, Columbia, Missouri 65201, personal communication). L. Stoch contributed a kaolinite from Janina, Poland, that had a higher than normal temperature of dehydroxylation (Stoch *et al.*, 1979). The Pugu, Tanganyika, sample is a highly disordered kaolinite (Robertson *et al.*, 1954).

The dickite samples in this study were essentially the same set of samples used by Brindley and Porter (1978). Many were massive and inhomogeneous, as judged from their color. Powders were obtained by scraping the surface with a razor blade and then grinding the scrapings gently in water. The grain sizes of the dickites were coarser than those of the kaolinites. More rigorous grinding was avoided to prevent undesirable structural damage. The dickites from Nowa Ruda, Poland, were examined by Stoch (1964). The dickite from Schuylkill, Pennsylvania, was studied by Newnham (1961).

X-ray powder diffraction

Samples for X-ray powder diffraction (XRD) studies were packed in shallow cavities in glass slides to minimize preferred orientation. XRD patterns were made with a Philips diffractometer, using Ni-filtered $CuK\alpha$ radiation, mainly from 18° to 30°2θ at a scan rate of 0.5°2θ/min and a chart-recording rate of 1°2θ/inch. The position and width of the 002 reflection provided useful indications of the thickness of the kaolinite plates.

Electron paramagnetic resonance

EPR measurements at X band (≈ 9 GHz) and 98 K were carried out on the Georgia kaolinites using a Var-

ian E109 spectrometer equipped with a liquid nitrogen cooled Varian E231 cavity (TE102 mode). Powdered samples (50 mg) were packed into 3-mm length quartz sample tubes, and the EPR signal was obtained at 25 mW incident power and with 100 kHz magnetic field modulation. The first derivative signal was stored in a MINC-11 minicomputer system and averaged over ten successive scans. The data were analyzed with a least-squares iterative computer program, run on a VAX 11/780 computer system.

The analysis is based on a least-squares iterative fit of the line intensity spectrum, obtained by integrating the first derivative signal, to a sum of four Gaussians representing lines at g_I, g_x, g_y, and g_z. The considerations underlying the procedure are: (1) The asymmetry of the EPR lineshape for a randomly oriented powder sample is greatly reduced as the linewidth increases. The component linewidths, at half height, in kaolinite are on the order of at least 100 gauss. (2) The I line, an isotropic line, is considered to have a Gaussian lineshape. Thus, any error in this procedure arose from the extent to which the components of the E line were asymmetric rather than Gaussian.

Fourier-transform infrared spectroscopy

IR spectra were obtained on a Digilab FTS-15E Fourier-transform infrared (FTIR) spectrometer which was optimized for the spectral range 4000 to 400 cm⁻¹. The pressed KBr pellet technique was used. One milligram (for kaolinite) or three milligrams (for dickite) of clay, taken from the bottle in the "as supplied" condition, was added to 200 mg of ground KBr. The mixture was gently stirred for about 1 min by a pestle in a mortar without exerting any pressure that could disorder the clay material. After drying overnight at 105°C, the mixture was placed in a pellet die, evacuated for 3 min, and pressed under vacuum at 7.4 kbar pressure over a 13-mm circular sample area. The resulting pellet was uniformly transparent to the eye. The larger sample concentration required for dickite, as compared to kaolinite, was due to the generally low absorbance of the dickite samples over the entire frequency range. Reduced sample concentrations were used for samples C and Nowa Ruda 1 (Table 3) to avoid spectral distortion due to high absorption beyond the linear range.

Two hundred scans at a resolution of 2 cm⁻¹ were signal averaged. The frequency scale was calibrated internally with a reference helium-neon laser to an accuracy of 0.2 cm⁻¹. The reported precision in the measured frequencies is 1 cm⁻¹. Each spectrum was deconvoluted into the different components in the frequency range of interest using a least-squares iterative fitting program on a minicomputer. The lineshape used in this program was a weighted fraction of a Gaussian and a Lorentzian profile, the fraction being refined by iteration. A good fit to all of the spectra was obtained with a pure Lorentzian profile.

Particle size, total iron content, and cation-exchange capacity

Particle-size analysis curves were obtained by the Centrifugal-Casagrande-Hydrometer Method (Norton and Speil, 1938). Total Fe_2O_3 was obtained colorimetrically. Cation-exchange capacities of all the kaolinite samples were determined using NH_4^+ as the exchangeable cation.

RESULTS

Particle size distribution

Particle-size analysis curves generally plot the weight percentage of a sample finer than given values in terms of equivalent spherical diameters of particles. To obtain a single number that represents the distribution of sizes, the following ratio was calculated as a particle size index:

$$\text{Particle size index} = \frac{\text{wt. \% } > 1.0 \ \mu m}{\text{wt. \% } < 1.0 \ \mu m}$$

The actual particle size indexes, as shown in Table 1, ranged from 65.7 to 0.028, i.e., 98.5% >1.0 μm for a coarse-grained kaolinite to 2.7% >1.0 μm for a fine-grained kaolinite. The use of the 1.0-μm particle size to obtain this ratio is arbitrary.

Hinckley index vs. particle size distribution

Hinckley indexes (Hinckley, 1963) of "crystallinity" are listed in Table 1. Although Hinckley indexes are only *semi-quantitative* measures, as contrasted with the *quantitative* measure of disorder achieved by Plançon and Tchoubar (1977a, 1977b) by computer fitting of XRD peak profiles, they are convenient for assigning a numerical value for the degree of structural disorder.

Figure 1 shows the Hinckley indexes of samples from the Georgia Kaolin Company plotted against the log of the particle size index. The particle size index of samples from the five localities varied considerably, but the Hinckley indexes were about the same for all clays from a given locality. A slight decrease in Hinckley index as the particle size index increased was indicated for the well-ordered clays from localities I, II, and English. In judging the data for the samples from localities IV and V, it must be recognized that the Hinckley index was only estimated to about ±0.05. Thus, the Hinckley indexes estimated for samples G and H were essentially the same, 0.25 ± 0.05 and, similarly, 0.35 ± 0.03 for samples L and M.

Total iron content

Two lines of evidence suggest that most of the iron in the Georgia kaolins is structural. Analysis of large numbers of samples, routinely performed by the Georgia Kaolin Company (private communication to J. L. Harrison), for both total iron and HCl-soluble iron has demonstrated that the amount of soluble iron ranges

Table 1. Sources, total Fe_2O_3, particle size indexes, and Hinckley indexes of kaolinites and dickites studied.

Locality	Sample	Particle size index	Fe_2O_3 (%)	Hinckley index	Supplied by
Kaolinites					
Keokuk, Iowa	KKK			1.54	W. D. Keller
Shelbina, Missouri	SHL			1.72	W. D. Keller
Janina, Poland (5–15 μm)	JAN			1.06	L. Stoch
I Wilkinson County, Georgia	B	0.06	0.31	1.52	
	C	0.18	0.27	1.57	
	A	0.79	0.26	1.44	
	I-MP	65.70	0.18	1.21	
English—Cornwall, Great Britain	E-3	0.14	0.48	1.16	
	E-2	0.16	0.43	1.14	
	E-1	0.61	0.42	1.14	
	E-MP	15.67	0.87	1.08	
II Twigg County, Georgia	E	0.06	0.20	1.15	
	F	0.17	0.22	1.09	Georgia Kaolin Company
	D	0.59	0.23	1.00	
	II-MP	19.00	0.26	0.81	
III Washington County, Georgia	J	0.07	0.99	0.41	
	K	0.09	0.99	0.43	
	I	0.29	1.02	0.43	
	III-MP	2.51	1.17	0.57	
IV Warren County, Georgia	L	0.05	1.11	0.32	
	M	0.11	1.15	0.38	
V Washington County, Georgia	G	0.03	1.07	0.18	
	H	0.04	1.08	0.31	
Pugu, Tanganyika	PUGU			0.24	G. W. Brindley
Dickites					
Jamaica 2 (pink)	J2			0.26	
Jamaica 3 (purple)	J3			0.28	G. W. Brindley
Jamaica 1 (green)	J1			0.29	
Nowa Ruda 1, Poland	NR1			0.61	
Nowa Ruda 2, Poland	NR2			0.87	A. Wiewiora
Jamaica 7 (white)	J7			1.00	G. W. Brindley
Red Mountain, Ouray, Colorado	RM			1.16	Ward's Natural Science Establishment, Inc.
Schuylkill, Pennsylvania (<350 mesh)	SCH			1.54	G. W. Brindley

between 5 and 15% of the total iron content. Selective dissolution of kaolins has shown also that iron and aluminum are removed at the same rate, strongly suggesting that the iron is located in octahedral sites in the kaolinite structure (J. L. Harrison, unpublished).

Figure 2 is a plot of % Fe_2O_3 vs. particle size index. For each locality, the % Fe_2O_3 values are reasonably constant, except for the coarse MP clays from localities III and English. These samples contain appreciable mica which probably accounts for these high iron values.

Comparison of Figures 1 and 2 suggests an inverse relation between the Hinckley index and the iron content. Although the data do not plot on a smooth curve, total iron content and degree of disorder tend to be directly related as indicated by the dashed bounding lines of Figure 3.

Cation-exchange capacity

With the exception of samples IIIMP and G to J, the cation-exchange capacities (CEC) of the kaolinites were in the range 2–6 meq/100 g. No correlation be-

tween Hinckley index and CEC was noted. The somewhat higher CEC value of 7.7 for sample IIIMP could be due to mica impurity. Samples G to K had CEC values in the range 9.8–12.2 meq/100 g; however, XRD data indicated the presence of smectite impurity, ≈10% for samples I to K and about half that for samples G to H.

Electron paramagnetic resonance

The EPR line intensity spectra were deconvoluted, as discussed above, into four Gaussian peaks centered at g_I, g_x, g_y, and g_z by a least-squares iterative fitting routine. The average g values and linewidths (at half height) derived from the deconvolution procedure for the five sets of Georgia samples are given in Table 2. It should be noted that the actual spread of g values for all thirteen Georgia samples was only 1.2% for g_I, 3.6% for g_x, 6.4% for g_y, and 4% for g_z. The r.m.s. deviation of the linewidth values within a given locality group in Table 2 was about 10%, except for the g_y component where it approached 15%. The data of Ta-
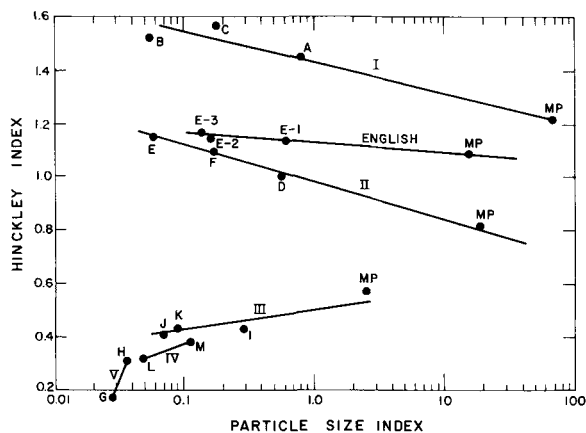
Figure 1.   Plot of Hinckley index vs. log of particle size index for Georgia and Cornwall kaolinites.

Figure 3.   Plot of % total Fe_2O_3 vs. Hinckley index. Dashed lines indicate approximate outer bounds of trend line.

ble 2 indicate that the width of the I line was significantly broader for the highly disordered samples as, indeed, would be expected. The good agreement between the g values of Table 2 and the literature values for kaolinite, the small spread in g values, and the reasonable values and degree-of-disorder dependence of the linewidths all reinforce the validity of the deconvolution procedure.

In Figure 4, the normalized (arbitrary scale) areas of the I and E lines for the suite of Georgia kaolinites are plotted against the respective Hinckley index values. The plots resemble that of Figure 3 for the total iron content; the inverse correlations between I and E areas and Hinckley index are similar to that between the total iron content and the Hinckley index. In Table 2 the fraction of total EPR spectral area due to the I line for each of the Georgia kaolinites is listed. The I area fraction increases significantly with increasing degree of disorder, as has been reported in the literature; however, the I area fraction is appreciable even for the
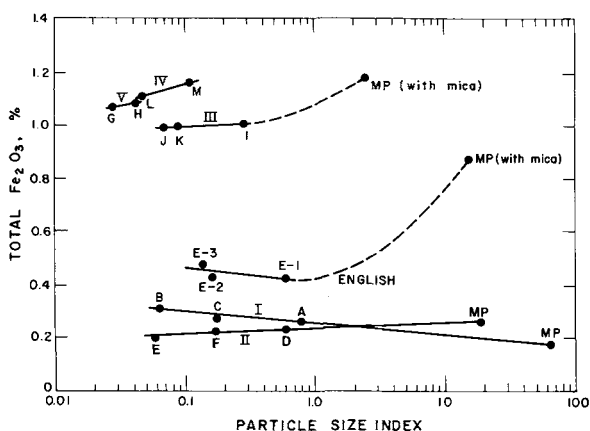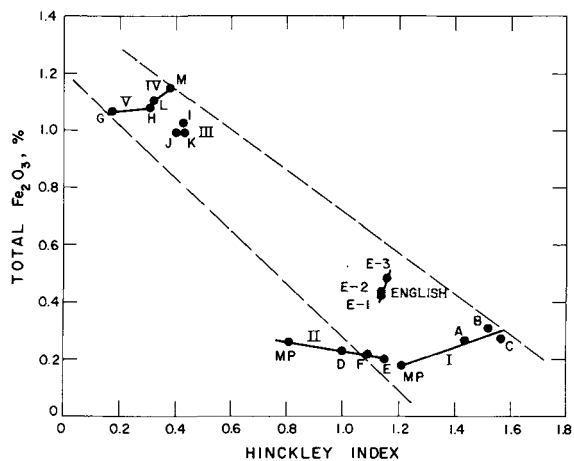
most well-ordered kaolinites which are low in total iron. This result is in disagreement with the claim of Mestdagh *et al.* (1980) that only the E signal is important in the EPR spectra of kaolinites containing small amounts of iron.

Fourier-transform infrared spectroscopy

As shown in Figure 5, four bands occur in the IR spectra of kaolinites at about 3700, 3670, 3650, and 3620 cm^{-1}, labeled ν_1, ν_2, ν_3, and ν_4, respectively, and three in dickites which correspond to ν_1, –, ν_3, and ν_4. A clear but weak band at about 3600 cm^{-1} was also present in the spectra of the disordered kaolinites K, M, H, and Pugu. Table 3 shows the results of deconvolution of spectra using the Lorentzian function to fit the bands. The frequencies of the peaks changed in a sequential manner from well-ordered kaolinites to well-ordered dickite via disordered intermediate states. The use of the terms ν_1, ν_2, ν_3, and ν_4 implies that the frequencies of the peaks were identified throughout the order-disorder range.

From Table 3, it is evident that samples of the Keokuk, Shelbina, and Janina kaolinites and many of the dickites gave unexpectedly low absorbances over the whole frequency range. The general shape of the spectra of the Keokuk, Shelbina, and Janina samples was different from those of other kaolinite samples, the bands being broader and the intensity (height) of band ν_1 smaller. Spectra of different samples from the same locality with different particle-size distributions, not presented here, also showed the same characteristic band broadening and low intensity (height) of band ν_1 for samples with coarse particle size distributions. Therefore, the difference in the shape of the spectra of Keokuk, Shelbina, and Janina kaolinites were probably due to wide particle size distributions.

Figure 6 shows the frequency of ν_1 vs. Hinckley index. Figure 7 shows the half-width of band ν_4 vs. Hinck-

Figure 2.   Plot of % total Fe_2O_3 vs. log of particle size index.

Table 2. Electron paramagnetic resonance data for the Georgia kaolinites.

Locality	Sample	Hinckley index[1]	Fractional I area[2] (%)	g_j[1]	Δ[3] (gauss)	g_x[1]	Δ[3] (gauss)	g_y[1]	Δ[3] (gauss)	g_z[1]	Δ[3] (gauss)
I	A		41.8								
	B	1.51	35.3	4.19	187	3.79	243	3.42	349	4.61	139
	C		39.8								
II	D		33.4								
	E	1.08	39.9	4.21	177	3.83	225	3.48	341	4.63	125
	F		39.9								
III	I		44.0								
	J	0.42	45.5	4.19	244	3.73	258	3.35	379	4.69	165
	K		44.9								
IV	L		41.0								
	M	0.35	45.8	4.19	235	3.74	246	3.38	349	4.67	159
V	G		43.5								
	H	0.25	42.6	4.19	220	3.76	240	3.40	354	4.66	163

[1] Average for each locality.
[2] Fraction of the total EPR spectral area due to the I line.
[3] Width at half height, averaged for each locality.

ley index. Figure 8 shows the spectra of the Schuylkill and Keokuk samples at room and at liquid nitrogen temperatures.

DISCUSSION

The plots of Hinckley index vs. size index presented in Figure 1 show that the Hinckley index is largely independent of the particle size distribution. Evidently, the Hinckley index is sensitive primarily to some aspect of structural disorder which affects reflections of the type $02l$, $11l$, with $l = 0, 1, 2$, forming the "02 diffraction band." Thus, the kaolinites from each locality have a characteristic kind of internal structural disorder which is fairly constant within the suite of samples from a given locality and is largely independent of the particle size distribution. Samples from different localities show a wide range of disorder features. Disorder appears to be a function of the geological environment, especially conditions of sedimentation, subsequent diagenesis, and chemistry of solutions.

The kaolins of east-central Georgia are part of a belt of kaolin districts extending along the inner edge of the Coastal Plain from South Carolina, across Georgia, into Alabama. The kaolins of eastern Georgia are of both Upper Cretaceous age and Tertiary, probably mostly Eocene, age. The Georgia kaolins have had a complex history, and no theory of origin is universally accepted; however, most investigators agree that the kaolins or their parent materials were transported and that the kaolins were altered from preexisting rocks.

The Tertiary and Cretaceous kaolins differ from each other in a number of ways. Tertiary kaolins characteristically are of very fine particle size, narrow particle size distribution, low degree of crystal structure order, and high iron content. In contrast, Cretaceous kaolins are of larger particle size, wider particle size distribu-

tion, higher degree of crystal structure order, and lower iron content. The Cretaceous kaolins tend to vary more from deposit to deposit than do the Tertiary kaolins. Georgia kaolinites from localities I and II are Cretaceous in age, and those from localities III, IV, and V are Tertiary in age. Table 1 shows that samples from localities I and II have Hinckley indexes >1.0 and those from localities III, IV, and V have Hinckley indexes <0.5. The samples labeled English are from the Cornwall district of Great Britain and are probably of hydrothermal origin. The differences in the geologic history of the Tertiary and Cretaceous kaolins are not well known, but the differences in the degree of disorder as well as other characteristics of the two ages of kaolins strongly suggest different environments of formation. In addition, the Tertiary kaolins were probably not developed from Cretaceous kaolin deposits.

A well-known trend in kaolinites exists that links an increase in total iron content with a decrease in degree of order. This relationship is usually regarded as exponential, and Figure 3 confirms this trend for the suite of Georgia samples (A to M), even allowing for a possible excess of iron in samples I to K due to smectite impurity. When, however, only the well-ordered samples (A to F) were considered, no correlation was found between total iron content and degree of order: samples D, E, and F from locality II were considerably more disordered than samples A, B, and C from locality I and yet had comparable iron contents. Thus, the claim of Mestdagh *et al.* (1982) that the introduction of Fe^{3+} into the octahedral layer leads to displacement of the octahedral vacancy and reduced degree of order is not substantiated by these well-ordered samples. As discussed below, the EPR data did not support this claim either.
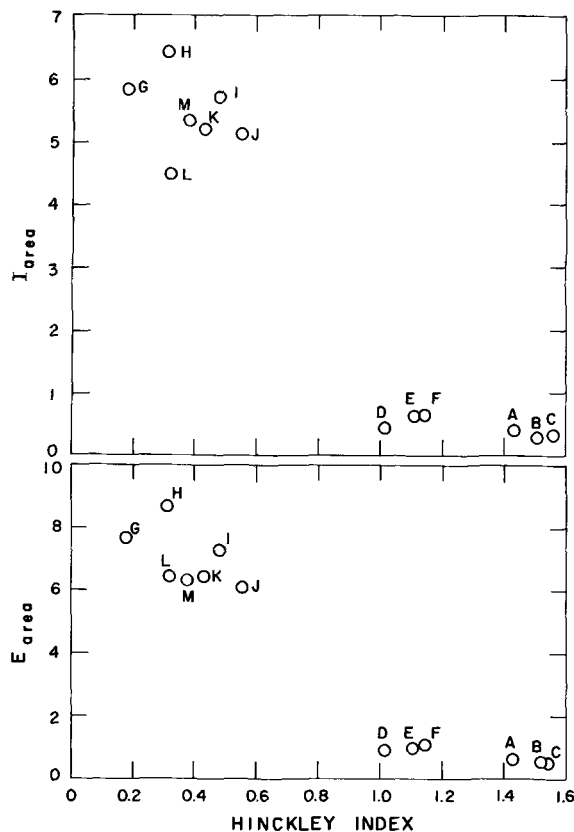
The EPR derivative spectrum of Georgia kaolinite

Figure 4. Plot of normalized (arbitrary scale) areas of I and E lines vs. Hinckley index for Georgia kaolinites.

Figure 5. Infrared spectra of kaolinites and dickites in hydroxyl-stretching band region.

sample E and its corresponding line intensity spectrum, obtained by integration, is shown in Figures 9a and 9b. The objective of the spectral analysis was to determine the relative area of the I line, where the relatively narrow feature (Figure 9a) centered in the neighborhood of 1550 gauss was largely due to this component. Figure 9c illustrates the analysis procedure used by Mestdagh *et al.* (1980, 1982) in their studies of the relationship between degree of disorder of kaolinite and the Fe^{3+} EPR spectrum. Their procedure is arbitrary and, undoubtedly, included in the "I area" some contribution from the E component. Furthermore, for highly disordered samples, e.g., sample L, the procedure could not be carried out, as illustrated in Figure 9d. The data of Table 2 show that the I area fraction did not fall below 33% even for sample D which contained only 0.23% total Fe_2O_3. The assumption of Mestdagh *et al.* (1982) that the EPR spectrum of samples containing less than about 0.5% Fe_2O_3 has a negligible I line contribution, which underlies the entire analysis of their EPR data, clearly did not hold with respect to the present samples. It should also be noted that the I line area fraction for sample E, for example, was 39.9% as determined from the deconvolution procedure and 54.2% as determined from the procedure of Mestdagh *et al.*
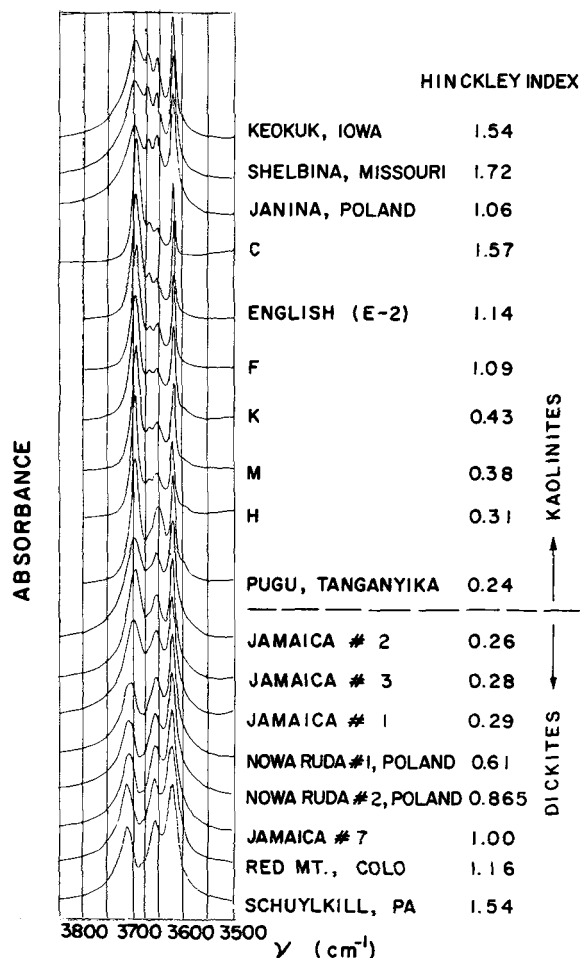
(1980, 1982). As indicated above, their procedure tends to overestimate the I line area. Furthermore, the data of Table 2 give a clear indication of a broadening of the I line which correlates (within experimental error) with increasing disorder.

In summary, the EPR data on the suite of Georgia kaolinites indicate that increasing total amounts of Fe_2O_3 and increasing fractional I area correlated with decreasing degree of order, as has been reported in the literature. Insofar as actual I and E areas are concerned, however, *both* correlated inversely with degree of order as shown in Figure 4, and the I area was appreciable even for samples having a low total iron concentration. The I line became broader with increasing disorder.

In well-ordered kaolinite four distinct hydroxyl-stretching bands were observed between 3700 cm⁻¹ and 3620 cm⁻¹. Ledoux and White (1964a, 1964b) showed that the three higher frequency bands (ν_1, ν_2, and ν_3) are due to the three inner-surface hydroxyls and that the ν_4 band at about 3620 cm⁻¹ is due to the inner

Table 3. Deconvolution of infrared spectra using the Lorentzian function to fit the bands.

Sample	Hinckley index	mg sample/200 mg KBr	Band 1			Band 2		
			Location	Intensity	Width[1] (cm^{-1})	Location (cm^{-1})	Intensity	Width[1] (cm^{-1})
KKK	1.54	1.0	3693	47.5	62.3	3669	11.3	8.0
SHL	1.72	1.0	3692	47.9	75.6	3669	10.7	7.9
JAN	1.06	1.0	3696	22.0	74.8	3669	4.2	6.0
C	1.57	0.75	3693	144.2	19.4	3668	21.1	12.0
E-2	1.14	1.0	3695	150.4	21.0	3669	23.3	11.3
F	1.09	1.0	3695	152.0	19.4	3670	16.5	9.7
K	0.43	1.0	3697	72.1	20.7	3670	5.6	7.4
M	0.38	1.0	3696	129.5	18.1	3670	10.8	7.9
H	0.31	1.0	3696	112.4	16.6	3670	8.8	8.3
PUGU	0.24	1.0	3698	55.4	19.3			
J2	0.26	3.0	3698	53.4	53.6			
J3	0.28	3.0	3697	94.0	42.1			
J1	0.29	3.0	3700	73.5	50.6			
NR1	0.61	2.7	3707	69.6	45.3			
NR2	0.87	3.0	3711	50.6	40.7			
J7	1.00	3.0	3710	54.0	39.0			
RM	1.16	3.0	3713	25.9	42.1			
SCH	1.54	3.0	3713	34.0	39.4			

Sample	Band 3			Band 4		
	Location (cm^{-1})	Intensity	Width[1] (cm^{-1})	Location (cm^{-1})	Intensity	Width[1] (cm^{-1})
KKK	3651	22.9	15.5	3620	54.3	12.5
SHL	3651	21.1	13.2	3619	54.7	12.3
JAN	3652	11.5	16.8	3620	29.0	14.6
C	3652	29.7	25.1	3620	85.5	7.2
E-2	3653	37.1	24.1	3620	113.2	6.8
F	3653	45.8	29.2	3620	107.5	7.5
K	3654	26.0	41.9	3621	49.4	9.7
M	3653	43.0	34.8	3621	82.5	8.8
H	3653	35.5	33.4	3621	62.7	9.3
PUGU	3653	32.3	32.6	3622	42.7	11.8
J2	3653	31.6	28.7	3621	55.8	21.1
J3	3652	57.2	28.2	3621	94.3	15.9
J1	3654	50.0	29.6	3621	83.2	20.6
NR1	3655	63.3	27.9	3621	108.4	23.2
NR2	3656	48.1	26.1	3621	82.5	26.9
J7	3656	51.2	25.9	3623	81.3	27.5
RM	3658	22.4	26.2	3622	40.7	29.9
SCH	3657	30.1	24.9	3622	56.5	29.8

[1] At half height.

hydroxyl. The 3620 cm^{-1} band in dickite was also considered to arise from the inner hydroxyl, although no proof of this assignment was given. It is well known that, in general, the hydroxyl-stretching frequency is displaced to lower frequency when hydrogen bonding is present. Adams (1983) found that the inner hydroxyls of kaolinite and dickite have very weak hydrogen bonding character. Surprisingly, no explanations have been published as to why the frequency of the inner-hydroxyl stretching band is lower than the frequencies of the stretching bands of the more strongly hydrogen-bonded, inner-surface hydroxyls.

It is generally accepted that ν_1 and ν_2 (at about 3700 and 3670 cm^{-1}) are, respectively, in-phase and out-of-phase combinatorial bands (Farmer and Russell, 1964; Farmer, 1964). The assignment of the ν_3 band (at about 3650 cm^{-1}) is controversial. Farmer and Russell (1964) suggested that ν_3 resulted from the three-fold symmetry

of the inner-surface hydroxyls not being exact. Rouxhet *et al.* (1977) claimed that this band was due to the fact that the orientation of one of the three hydroxyls is almost perpendicular to the other two. This explanation is untenable, however, in light of the recent refinement of the crystal structure of kaolinite (Suitch and Young, 1983) which shows that all three inner-surface hydroxyls are equally involved in the hydrogen bonding between kaolinite layers. On the other hand, Prost (1984) found evidence for four distinct bands in Ouray dickite at 7 K lying beyond 3654 cm^{-1}, in addition to the ν_3 and ν_4 bands at 3654 and 3618 cm^{-1}. The band assignment of Farmer and Russell (1964) thus appears to be incomplete, at least insofar as dickite is concerned.

The plot of the ν_1 band frequency vs. Hinckley index (Figure 6) for the entire suite of kaolinites and dickites shows a sequential increase in frequency in passing
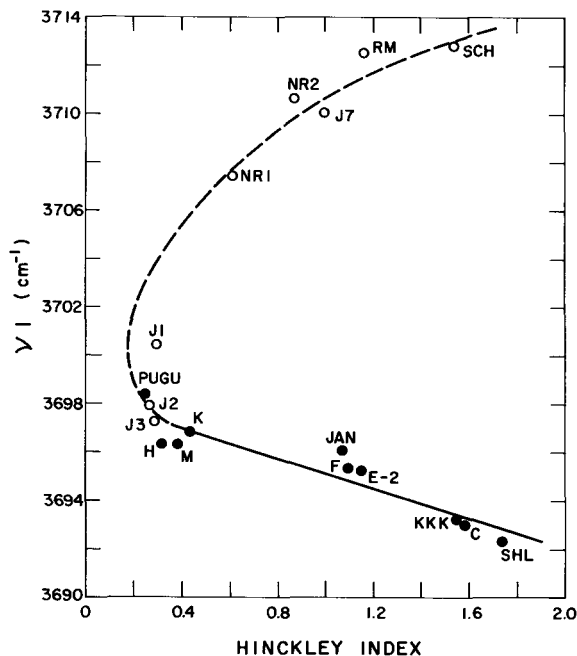
Figure 6. Plot of frequency of band ν_1 vs. Hinckley index.
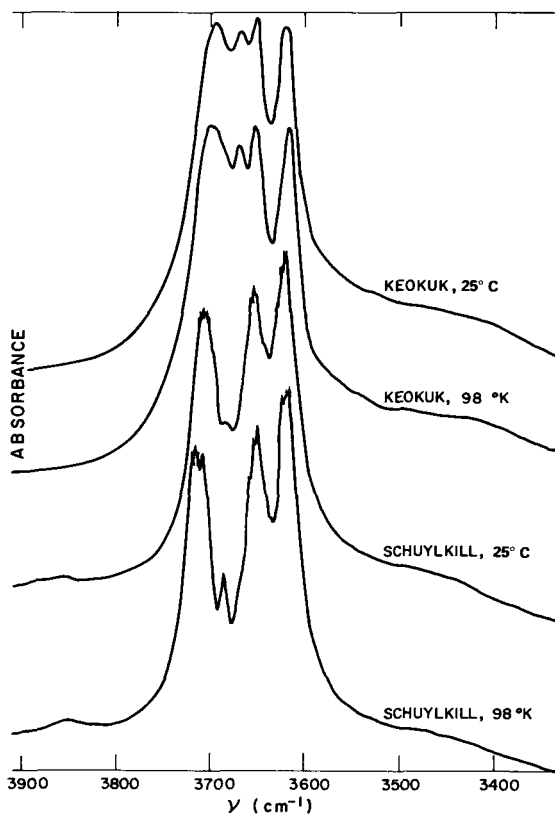

Figure 8. Infrared spectra of Schuylkill and Keokuk samples at room temperature and at liquid nitrogen temperature.
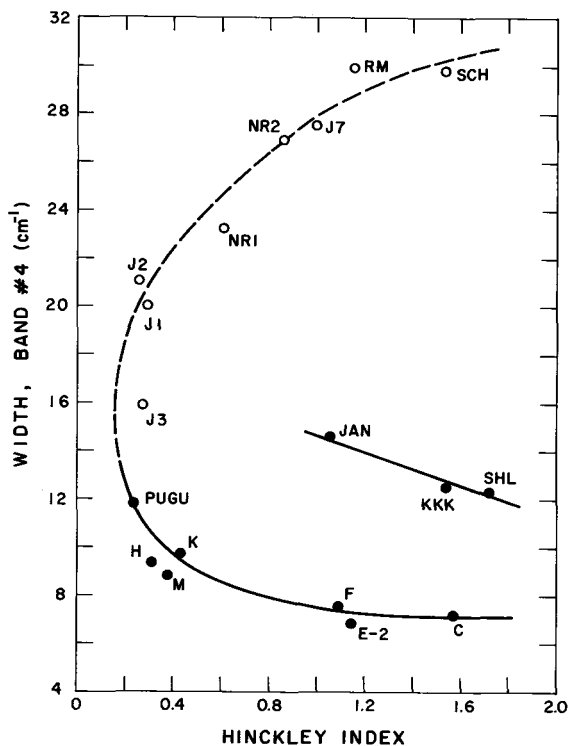

Figure 7. Plot of half-width of band ν_4 vs. Hinckley index.

from well-ordered kaolinite through the disordered structures to well-ordered dickite. A similar sequential increase was observed (Table 3) in the ν_2 and ν_3 frequencies although it was difficult to delineate at room temperature the ν_2 band in many of the dickites. At 98 K (Figure 8) the ν_2 band of well-ordered dickite was clearly delineated and was at a greater frequency than the ν_2 band for well-ordered kaolinite. The higher values for the stretch frequencies of the inner-surface hydroxyls in dickite, as compared to kaolinite, indicate that the interlayer hydrogen bonding is weaker in dickite than in kaolinite. The lack of difference in the ν_1 frequency for very disordered kaolinite and very disordered dickite is consistent with the model for disorder based on vacancy displacement. From the point of view of the vacancy-displacement model, very disordered kaolinite cannot be distinguished from very disordered dickite; the vacancies in the former were randomly disordered between the B and C positions.

From Table 3 and Figure 8, it is clear that the frequency of band ν_4 was essentially constant for the entire suite of samples, and, furthermore, was practically independent of temperature. Prost (1984) also found little difference in the ν_4 frequency between Georgia kaolinite and Ouray dickite and little temperature dependence of ν_4 over a wide range of temperature. A constant frequency of the ν_4 band is reasonable inasmuch as the vibration frequency of the inner hydroxyl should not be expected to be sensitive to a long-range perturbation, such as the vacancy displacement from
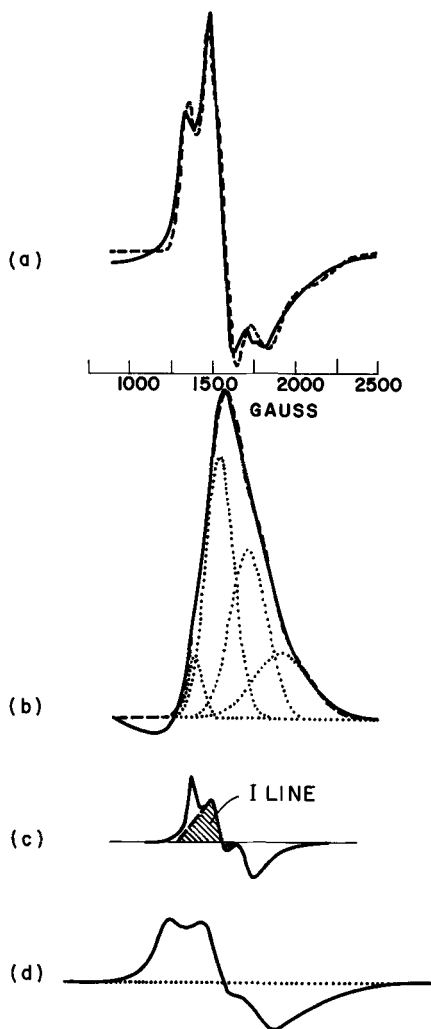
Figure 9. (a) Electron paramagnetic resonance derivative spectrum of Georgia kaolinite sample E. Dashed line is derivative of sum of the Gaussian components delineated in (b); (b) Corresponding line intensity spectrum obtained by integration. Dotted lines delineate four Gaussian components obtained from deconvolution; (c) Analysis procedure used by Mestdagh *et al.* (1980); (d) Electron paramagnetic resonance derivative spectrum of sample L, highly disordered sample.

one layer to the next. In fact, it is well known that the ν_4 vibration frequency is not affected by intercalation, i.e., by changes in the hydrogen bonding of the inner-surface hydroxyls. Figure 7, however, a plot of the width (at half height) of the ν_4 band vs. Hinckley index, shows a sequential increase in width in passing from well-ordered kaolinite through the disordered states to well-ordered dickite. Although some increase in bandwidth was expected due to the larger particle size of the dickites and the Shelbina, Keokuk, and Janina kaolinites, as is evidenced by the width of the ν_1 band (Table 3), the increased bandwidth of ν_4 did not appear to be dominated by this effect. In fact, the bandwidths

of ν_4 increased with decreasing Hinckley index even within the suite of Georgia kaolinites, where the particle size effectively decreased with disorder. Thus, the frequency of the ν_4 band was insensitive to disorder and changed little with temperature, but the bandwidth increased as a function of . . .BC. . . character to a maximum for well-ordered dickite.

The refined crystal structure of kaolinite and dickite (Suitch and Young, 1983) is incompatible with the observed character of the ν_4 band. Suitch and Young found that all the inner hydroxyls have the same orientation in dickite, whereas a double unit cell must be considered for kaolinite with the O–H directed into an octahedral vacancy in one half cell and towards the ditrigonal hole in the other half cell. It is therefore expected that kaolinite should exhibit two inner-hydroxyl vibration bands, or possibly a single broad band, with some temperature dependence (inasmuch as temperature probably perturbed the two vibration frequencies differently), whereas dickite should exhibit a single vibration band of normal width.

CONCLUSIONS

This study shows that kaolinites from different localities possess different degrees of internal structural disorder and characteristic ranges of total iron. These results were largely independent of particle size distribution and suggest a correlation with geological and geochemical factors.

EPR spectra showed that the intensity of the isotropic (I) line was significant even at low total iron concentrations. The intensities of both the I and E lines increased with increasing disorder as did the width of the I line.

IR studies showed a sequential increase in the inner-surface, hydroxyl-stretching band frequency in passing from well-ordered kaolinite to well-ordered dickite, indicating that the interlayer hydrogen bonding is weaker in dickite than in kaolinite. Furthermore, no difference in the ν_1 frequency for very disordered kaolinite and very disordered dickite was noted, consistent with a model for disorder based on vacancy displacement.

The frequencies and bandwidths of the ν_4 stretching band of the inner hydroxyl were found to be in striking disagreement with what was to be expected on the basis of the most recent refinement of the crystal structures of kaolinite and dickite (Suitch and Young, 1983). The ν_4 band frequency was essentially constant and temperature independent. The bandwidth showed a sequential increase in passing from well-ordered kaolinite to well-ordered dickite, the increase being considerably in excess of any broadening due to increased particle size. We conclude that the frequency, temperature dependence, and bandwidth of the ν_4 band of the inner hydroxyl in kaolinites and dickites are not understood at this time.

ACKNOWLEDGMENTS

REFERENCES

Adams, J. M. (1983) Hydrogen atom positions in kaolinite by neutron profile refinement: *Clays & Clay Minerals* **31**, 352–356.

Adams, J. M. and Hewat, A. W. (1981) Hydrogen atom positions in dickite: *Clays & Clay Minerals* **29**, 316–319.

Angel, B. R., Jones, J. P. E., and Hall, P. L. (1974) Electron spin resonance studies of doped synthetic kaolinite. I: *Clay Miner.* **10**, 247–255.

Bailey, S. W. (1963) Polymorphism of the kaolin minerals: *Amer. Mineral.* **48**, 1196–1209.

Brindley, G. W. and Nakahira, M. (1958) Further considerations of the crystal structure of kaolinite: *Mineral. Mag.* **31**, 781–786.

Brindley, G. W. and Porter, A. R. D. (1978) Occurrence of dickite in Jamaica: ordered and disordered varieties: *Amer. Mineral.* **63**, 554–562.

Brindley, G. W. and Robinson, K. (1946) The structure of kaolinite: *Mineral. Mag.* **27**, 242–253.

Cruz-Cumplido, M., Sow, C., and Fripiat, J. J. (1982) Spectre infrarouge des hydroxyles, cristallinité et énergie de cohésion des kaolins: *Bull. Mineral.* **105**, 493–498.

Farmer, V. C. (1964) Infrared absorption of hydroxyl groups in kaolinite: *Science* **145**, 1189–1190.

Farmer, V. C. and Russell, J. D. (1964) The infrared spectra of layer silicates: *Spectrochim. Acta* **20**, 1149–1173.

Giese, R. F., Jr. (1982) Theoretical studies of the kaolin minerals. Electrostatic calculations: *Bull. Mineral.* **105**, 417–424.

Giese, R. F., Jr. and Datta, P. (1973) Hydroxyl orientation in kaolinite, dickite and nacrite: *Amer. Mineral.* **58**, 471–479.

Hall, P. L. (1973) Electron spin resonance studies of aluminasilicate minerals and associated organic substances: Ph.D. thesis, University of London, 209 pp.

Hinckley, D. N. (1963) Variability in "crystallinity" values among the kaolin deposits of the coastal plain of Georgia and South Carolina: in *Clays and Clay Minerals, Proc. 11th Natl. Conf., Ottawa, Ontario, 1962,* Ada Swineford, ed., Pergamon Press, New York, 229–235.

Jones, J. P. E., Angel, B. R., and Hall, P. L. (1974) Electron spin resonance studies of doped synthetic kaolinite. II: *Clay Miner.* **10**, 257–270.

Keller, W. D., Pickett, E. E., and Reesman, A. L. (1966) Elevated dehydroxylation temperature of the Keokuk geode

kaolinite: in *Proc. Inter. Clay Conf., Jerusalem, 1966, Vol. 1,* L. Heller and A. Weiss, eds., Israel Prog. Sci. Trans., Jerusalem, 75–85.

Ledoux, R. L. and White, J. L. (1964a) Infrared study of selective deuteration of kaolinite and halloysite at room temperature: *Science* **145**, 47–49.

Ledoux, R. L. and White, J. L. (1964b) Infrared studies of the hydroxyl groups in intercalated kaolinite complexes: in *Clays and Clay Minerals, Proc. 13th Natl. Conf., Madison, Wisconsin, 1964,* W. F. Bradley and S. W. Bailey, eds., Pergamon Press, New York, 289–315.

Meads, R. E. and Malden, P. S. (1975) Electron-spin resonance in natural kaolinites containing Fe^{3+} and other transition metal ions: *Clay Miner.* **10**, 313–345.

Mestdagh, M. M., Herbillon, A. J., Rodrique, L., and Rouxhet, P. G. (1982) Evaluation du rôle du fer structural sur la cristallinité des kaolinite: *Bull. Mineral.* **105**, 457–466.

Mestdagh, M. M., Vielvoye, L., and Herbillon, A. J. (1980) Iron in kaolinite: II. The relationship between kaolinite crystallinity and iron content: *Clay Miner.* **15**, 1–13.

Newnham, R. E. (1961) A refinement of the dickite structure and some remarks on polymorphism in kaolin minerals: *Mineral. Mag.* **32**, 683–704.

Newnham, R. E., and Brindley, G. W. (1956) The crystal structure of dickite: *Acta Crystallogr.* **9**, 759–764.

Newnham, R. E. and Brindley, G. W. (1957) The structure of dickite: correction: *Acta Crystallogr.* **10**, 88.

Norton, F. H. and Speil, S. (1938) The measurement of particle sizes in clays: *J. Amer. Ceram. Soc.* **21**, 89–97.

Plançon, A. and Tchoubar, C. (1977a) Determination of structural defects in phyllosilicates by X-ray powder diffraction — I. Principle of calculation of the diffraction phenomenon: *Clays & Clay Minerals* **25**, 430–435.

Plançon, A. and Tchoubar, C. (1977b) Determination of structural defects in phyllosilicates by X-ray powder diffraction — II. Nature and proportion of defects in natural kaolinites: *Clays & Clay Minerals* **25**, 436–450.

Prost, R. (1984) Etude par spectroscopie infrarouge à basse température des groupes OH de structure de la kaolinite, de la dickite et de la nacrite: *Agronomia* **4**, 403–406.

Robertson, R. H. S., Brindley, G. W., and Mackenzie, R. C. (1954) Mineralogy of kaolin clays from Pugu, Tanganyika: *Amer. Mineral.* **39**, 118–139.

Rouxhet, P. G., Samudacheata, N., Jacobs, H., and Anton, O. (1977) Attribution of the OH stretching bands of kaolinite: *Clay Miner.* **12**, 171–178.

Stoch, L. (1964) Thermal dehydroxylation of minerals of the kaolinite group: *Bull. Acad. Polon. Sci. Ser. Sci. Geol. Geogr.* **12**, 173–180.

Stoch, L., Rybicka, E., and Gorniak, K. (1979) Mineralogical composition of kaolinite clays from the "Janina" mine at Suszki near Boleslawiec: *Mineral. Polon.* **10**, 63–79.

Suitch, P. R. and Young, R. A. (1983) Atom positions in highly ordered kaolinite: *Clays & Clay Minerals* **31**, 357–366.

Tchoubar, C., Plançon, A., Ben Brahim, J., Clinard, C., and Sow, C. (1982) Caractéristiques structurales des kaolinites désordonnées: *Bull. Mineral.* **105**, 477–491.

Zvyagin, B. B. (1960) Electron diffraction determination of the structure of kaolinite: *Kristallografiya* **5**, 32–41.